

Is manganese-doped diamond a ferromagnetic semiconductor?

Steven C. Erwin and C. Stephen Hellberg

Center for Computational Materials Science, Naval Research Laboratory, Washington, D.C. 20375

(Dated: November 21, 2018)

We use density-functional theoretical methods to examine the recent prediction, based on a mean-field solution of the Zener model, that diamond doped by Mn (with spin $S=5/2$) would be a dilute magnetic semiconductor that remains ferromagnetic well above room temperature. Our findings suggest this to be unlikely, for four reasons: (1) substitutional Mn in diamond has a low-spin $S=1/2$ ground state; (2) the substitutional site is energetically unfavorable relative to the much larger “divacancy” site; (3) Mn in the divacancy site is an acceptor, but with only hyperdeep levels, and hence the holes are likely to remain localized; (4) the calculated Heisenberg couplings between Mn in nearby divacancy sites are two orders of magnitude smaller than for substitutional Mn in germanium.

PACS numbers:

I. INTRODUCTION

A large class of dilute magnetic semiconductors (DMS) is based on manganese doping of III-V or group-IV hosts having the zincblende, wurzite, or diamond structure. Formally, Mn is either a single or double acceptor, depending on whether it substitutes for a group-III or -IV atom, respectively.^{1,2} Aside from this difference, there are no simple guidelines for predicting how the magnetic behavior of the resulting DMS depends on the choice of host semiconductor. Elucidating such guidelines would be of great practical interest for efforts to control and optimize the magnetic properties of DMS materials. In particular, it would be very helpful to understand how the resulting Curie temperatures depend on the choice of host semiconductor.

An important and early contribution was made by Dietl, who used a mean-field solution of the Zener model to predict the Curie temperatures for Mn doping of a wide range of II-VI, III-V, and group-IV host semiconductors.^{3,4} Mn ions with localized spin $S=5/2$ were assumed to substitute on the cation site, and to interact by an indirect exchange interaction mediated by holes. Curie temperatures were calculated for fixed Mn content $x = 5\%$ and hole concentration $p = 3.5 \times 10^{20} \text{ cm}^{-3}$ using the mean-field result

$$k_B T_C = x_{\text{eff}} N_0 S(S+1) \beta^2 A_F m^* k_F / 12 h^2. \quad (1)$$

In this equation, the most direct dependence of T_C on the host semiconductor comes from the density per unit volume of cation sites N_0 , which varies with the host lattice constant as $1/a^3$. A much weaker dependence on the host arises from the density-of-states effective mass m^* and the Fermi wavevector k_F . The remaining variables, i.e. the p - d exchange integral β and the Fermi-liquid parameter A_F , were assumed not to depend on the host.

The full numerical evaluation of Eq. (1) for different host semiconductors⁴ leads to values of T_C that indeed track the prefactor $1/a^3$ quite closely.⁵ For example, the hosts with the largest lattice constants (CdTe, InAs, Ge) lead to the smallest predicted Curie temperatures (be-

low $\sim 75 \text{ K}$). Likewise, the hosts with the smallest lattice constants (ZnO, GaN, C) lead to the largest predicted values of T_C (well above room temperature).

Diamond has the smallest lattice constant of all the semiconductors ($a = 3.56 \text{ \AA}$) and, accordingly, the highest predicted Curie temperature ($T_C \approx 470 \text{ K}$). These extreme values make diamond a logical choice for examining some of the assumptions underlying the predictions of high Curie temperatures for hosts having small lattice constants. In this paper, we use first-principles theoretical methods to test the assumption that Mn occupies the substitutional site, with spin $S = 5/2$, in the diamond lattice. We find that substitutional Mn has a low-spin $S=1/2$ ground state in diamond. Moreover, because of diamond’s small lattice constant, the substitutional site is energetically unfavorable relative to the much larger “divacancy site,” denoted V_2 , which we identify as the more likely Mn impurity location. We analyze the electronic and magnetic structure of this divacancy Mn impurity in diamond, and show that it is unlikely to lead to magnetic ordering at any reasonable temperature.

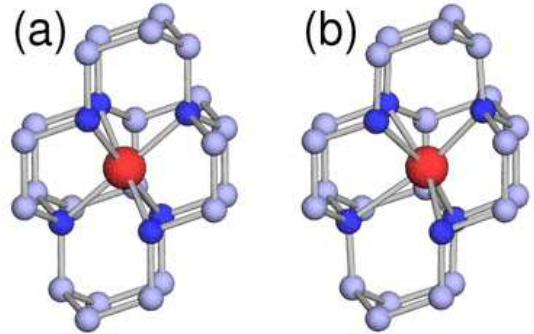


FIG. 1: (a) Ideal and (b) completely relaxed geometry of the Mn impurity in a diamond divacancy site.

II. METHODS

Most of the results reported in this article are for isolated Mn impurities, which we simulate using a supercell of 64 carbon atoms in the diamond structure. All atomic positions were relaxed using total energies and forces calculated within the generalized-gradient approximation to density-functional theory (DFT), as implemented in VASP.^{6,7} Carbon and Mn ultrasoft pseudopotentials were used with a cutoff energy of 286 eV. For total energies, we used $2 \times 2 \times 2$ Monkhorst-Pack sampling of the Brillouin zone, and $4 \times 4 \times 4$ sampling for convergence checks. In the discussion of the electronic structure of the isolated Mn impurity at a divacancy site, eigenvalues at the zone center of a 128-atom supercell are reported in order that degeneracies are properly represented.

Within the supercell formalism, the formation energy of a Mn impurity is given by

$$E_{\text{form}}[\text{Mn}^q] = E_t[\text{Mn}^q] - n_C \mu_C - \mu_{\text{Mn}} + q E_F, \quad (2)$$

where $E_t[\text{Mn}^q]$ is the total energy of a supercell containing n_C carbon atoms and one Mn impurity, with chemical potentials μ_C and μ_{Mn} , q is the charge state of the Mn impurity, and E_F is the Fermi level. Since the host crystal is elemental, the chemical potentials are simply the energy per atom in the diamond phase of carbon and the ground-state αMn .

The electrical activity of a Mn impurity is determined by its formation energy as a function of charge state. Electrically active defects will have more than one stable charge state within the host band gap; the value of E_F for which two such charge states have equal formation energies is referred to as a “charge transition level.” The charge transition level between the neutral and $q = +1$ states is the donor ionization energy, while the transition level between neutral and $q = -1$ states is the acceptor ionization energy. In practice, the total energy of a charged supercell must be calculated by adding a uniform compensating background charge to the supercell. The long-range nature of the Coulomb interaction then gives rise to a spurious Madelung-like contribution to the total energy, which must be subtracted from the calculated total energy. This was done using a standard approach in which a multipole expansion of the defect charge (up to quadrupole order) was used to estimate the interaction energy analytically and then subtract it off.⁸

The magnetic interaction between Mn impurities in nearby divacancy sites was calculated using larger supercells of 128 carbon atoms. No relaxations were performed for these calculations; tests for a few configurations confirmed that this approximation did not change the results significantly. The interactions are represented by numerically mapping the DFT total energies into the Heisenberg form. In practice this amounts to computing the difference in total energy between the parallel and antiparallel spin alignment of two Mn impurities in a supercell.

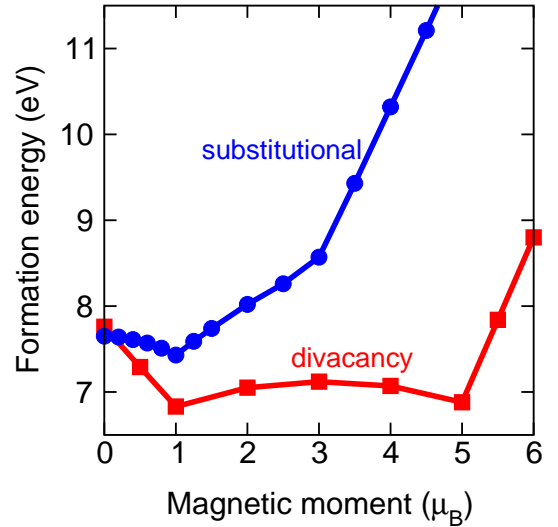


FIG. 2: Formation energy of substitutional and divacancy Mn in diamond, as a function of constrained magnetic moment.

III. ENERGETICS

The Mn impurity enjoys a special status as a dopant in dilute magnetic semiconductors such as $\text{Mn}_x\text{Ga}_{1-x}\text{As}$ and $\text{Mn}_x\text{Ge}_{1-x}$. It preferentially occupies the substitutional (cation) site, where it serves two roles: it is electrically active as an acceptor, and it contributes a localized spin $S = 5/2$. At sufficient Mn concentrations, holes are created in the host valence band; these delocalized carriers mediate the ferromagnetic interaction between the localized spins.^{3,4}

GaAs and Ge have similar lattice constants, and since strain contributes to the impurity formation energy, it is instructive to note that the local strain around a substitutional Mn impurity, denoted Mn_{sub} , is very small for both hosts—the nearest neighbors distort by less than 2% from their ideal positions. Tetrahedrally coordinated interstitial Mn impurities, denoted Mn_{tet} , have higher formation energies (by 1–2 eV for neutral impurities); interestingly, the atomic volume available at this site is the same as for the substitutional site, and consequently very little distortion is created by the Mn interstitial in either host.⁹

The lattice constant of diamond is 37% smaller than that of Ge, and so it is not surprising that a substitutional Mn impurity creates a much larger local strain in the lattice—within DFT the nearest-neighbor distortion is 12%. Because of the extreme stiffness of diamond, such a large strain is expected to lead to a relatively high formation energy. A similar distortion occurs for Mn in the tetrahedral interstitial site.

A simple way to relieve this strain is to place the Mn impurity at a divacancy site—i.e. to remove two neighboring carbon atoms and place the Mn at their midpoint, as shown in Fig. 1(a). This doubles the atomic volume available, leading to a much reduced local strain—

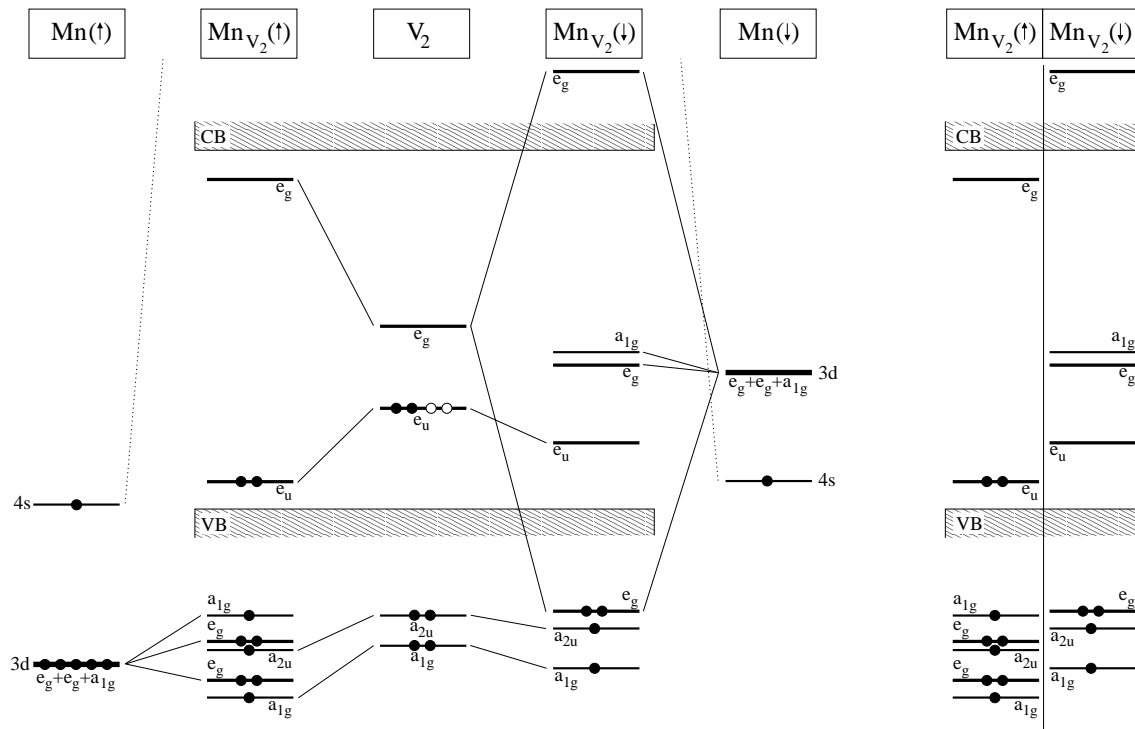


FIG. 3: Energy-level diagram for divacancy Mn impurity in diamond, MnV_2 . Left panels show how majority (\uparrow) and minority (\downarrow) levels arise from hybridization of Mn atomic states with diamond divacancy (V_2) states. Right panel summarizes the resulting energy levels.

only 2% distortion of the nearest neighbors. Even in its ground-state configuration, which includes a slight off-center relaxation of the Mn ion as shown in Fig. 1(b), the local lattice distortion around this MnV_2 impurity is very small. It is already widely believed that other large impurities—including Si, P, Ni, and Co—preferentially occupy the divacancy site in diamond;^{10,11,12,13,14} hence our prediction that Mn also prefers this site appears plausible.

To make the comparison between different sites quantitative we turn now to the formation energies calculated within DFT. For neutral Mn impurities, we find the divacancy site is strongly preferred (by 0.6 eV) to the substitutional site; the interstitial site is much less favorable than either (by ~ 10 eV). Figure 2 shows the formation energies for divacancy and substitutional Mn as a function of magnetic moment, calculated using the fixed-spin-moment method within DFT. Even in the preferred divacancy site, the absolute formation is almost an order of magnitude larger for substitutional Mn in GaAs or Ge, suggesting that standard methods for attaining high concentrations of magnetic dopants will probably not work for diamond.

The equilibrium magnetic moments M in the substitutional and divacancy sites are also quite different compared to substitutional Mn in GaAs and Ge ($M = 4$ and $3 \mu_B$, respectively). In the substitutional site, Mn adopts a low-spin $M = 1$ state, with an extremely small energy gain (0.1 eV) relative to the spin-unpolarized state.

Hence, we anticipate that even if Mn could be forced into the substitutional site, its magnetic moment may not be sufficiently stable to facilitate magnetic ordering. In the divacancy site two nearly degenerate moments are found ($M = 1$ and $5 \mu_B$) with an energy difference of only 0.05 eV; the formation energy vs. magnetic moment is symmetrical about $M = 3 \mu_B$. This peculiar feature of the MnV_2 impurity will be explained in Section IV.

IV. ELECTRONIC STRUCTURE

The MnV_2 impurity has an energy-level structure that arises from the relatively weak interaction of atomic Mn levels and host divacancy levels, as shown in Fig. 3. The host divacancy defect itself has been extensively studied both theoretically and experimentally, and is well understood.^{15,16,17,18} The removal of two carbon atoms from the host lattice leads to a defect with D_{3d} symmetry, and thus the six available dangling-bond orbitals must form linear combinations that transform under the irreducible representations a_{1g} , a_{2u} , e_u , and e_g .¹⁹ For the neutral divacancy, six electrons are available to fill these levels. In an early theoretical study, Coulson and Larkins²⁰ predicted the ground state one-electron configuration to be $a_{1g}^2 a_{2u}^2 e_u^2$. Later calculations confirmed this one-electron level ordering for both silicon and diamond, and we find it here too, as shown.

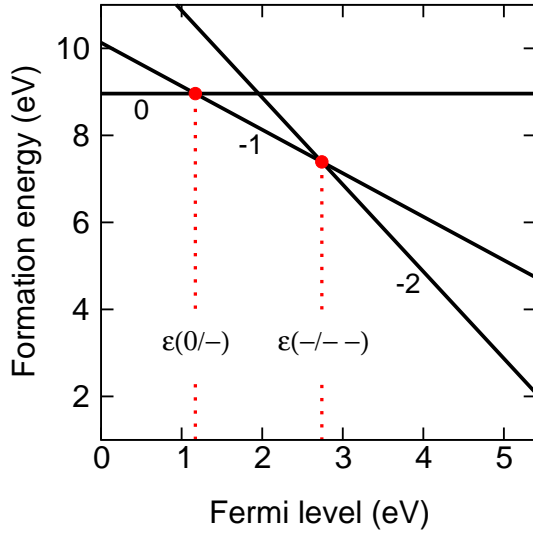


FIG. 4: Formation energy of divacancy Mn impurity in diamond, as a function of the Fermi level. Two charge-transition levels fall within the diamond band gap, as indicated.

In Fig. 3 we consider separately the interaction of the majority and minority Mn levels with the four divacancy levels. Under the D_{3d} crystal field, the $3d$ level of Mn splits into one a_{1g} and two e_g levels. Hence, hybridization is allowed only between Mn and V_2 levels both having either a_{1g} or e_g symmetry, but no mixing is allowed between Mn levels and V_2 levels having either a_{2u} or e_u symmetry. Among the calculated majority $Mn_{V_2}(\uparrow)$ levels we find very little mixing within any level, and therefore each has a clear parentage from either Mn or V_2 orbitals, as indicated in Fig. 3. For the minority $Mn_{V_2}(\downarrow)$ levels there is strong mixing between the empty V_2 e_g level and the empty Mn $e_g(\downarrow)$ level, so that the occupied bonding combination falls well below the diamond valence-band maximum (VBM). Considering for the moment only those levels that sit below the VBM, we find that seven electrons occupy majority levels and four electrons occupy minority levels. Hence, these low-lying levels carry a net “core” magnetic moment $M_{\text{core}} = 3\mu_B$.

The highest occupied molecular orbital (HOMO) of the Mn_{V_2} impurity has e_u symmetry and, because it cannot mix with Mn states, is purely derived from the V_2 dangling-bond orbitals. The two electrons in this four-fold level form a spin triplet ($M_{\text{HOMO}} = 1\mu_B$) as shown, but the system is energetically indifferent to whether they are aligned parallel or antiparallel to the core spin (Fig. 3 shows the parallel alignment; when the alignment is made antiparallel the spin-up and spin-down HOMO levels simply switch positions).

Because of this weak coupling between the HOMO spin and the core spin, the total magnetic moment of Mn_{V_2} can assume two possible low-energy values: either $M_{\text{core}} + M_{\text{HOMO}} = 5\mu_B$ or $M_{\text{core}} - M_{\text{HOMO}} = 1\mu_B$ for parallel or antiparallel alignment, respectively. Moreover, there is an energy penalty for violating Hund’s Rule

by forcing the HOMO into a spin-singlet state; this is the origin of the energy increase that occurs when the total moment is constrained to $3\mu_B$ (the core moment alone). These two features—the weak core-HOMO spin coupling, and the Hund’s Rule penalty for constraining the HOMO to a spin singlet—explain the unusual appearance, shown earlier in Fig. 2, of the Mn_{V_2} formation energy vs. total magnetic moment.

V. ELECTRICAL ACTIVITY

In Fig. 4 we show the calculated formation energies of Mn_{V_2} for charge states that are stable within the experimental 5.4-eV band gap of diamond. There are three such stable charge states ($q = 0, -1, -2$), making Mn_{V_2} formally a double acceptor. In principle this is similar to the case of substitutional Mn in Ge, which is also a double acceptor, and might suggest similar electrical activity for Mn_{V_2} .

Quantitatively, however, the two cases are quite different. The first two acceptor ionization energies for Mn in Ge have been measured experimentally to be 160 and 370 meV, relative to the valence-band edge.²¹ For Mn concentrations of several percent, the width of the resulting impurity band is sufficient to create overlap with the valence band and thus to allow the holes to delocalize. Likewise, Mn in GaAs is a single acceptor with a measured acceptor level at 113 meV,²² which is accurately given by DFT calculations as 100 meV.⁹

On the other hand, the predicted first acceptor ionization energy for Mn_{V_2} in diamond is an order of magnitude larger, $\epsilon(0/-) = 1.2$ eV, suggesting that the holes will remain localized on the impurity sites for any reasonable Mn concentration. For this reason alone, it appears very unlikely that there will be sufficient carriers to mediate a ferromagnetic interaction between the localized spins of Mn_{V_2} impurities.

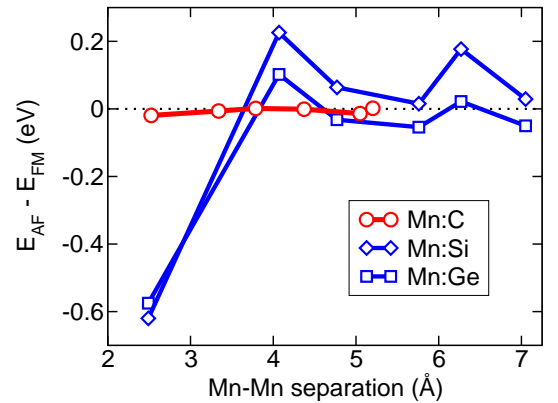


FIG. 5: Heisenberg spin-coupling constant between two Mn impurities in C (diamond), Si, and Ge host crystals. For diamond, Mn atoms are at divacancy sites; for Si and Ge, Mn atoms are on substitutional sites.

VI. MAGNETIC INTERACTIONS

The weak coupling between core and HOMO spins in the isolated Mn_{V_2} impurity suggests that the effective coupling between spins of two impurities will also be weak. This expectation is confirmed in Fig. 5, where we show the results of our DFT calculations for (twice) the Heisenberg coupling constant between two Mn_{V_2} impurities in a 128-atom diamond supercell. For comparison, we show the results of similar calculations for substitutional Mn in Ge and Si.

The results for substitutional Mn in Ge and Si show a similar trend. When the two Mn are nearest neighbors, there is a strong preference for antiparallel spin alignment. At larger separations the interactions vary in sign (Ge) and/or magnitude (Si), a consequence of the crystallographic anisotropy that arises from the strong d character of the acceptor wavefunction in substitutional Mn. The largest ferromagnetic coupling strengths are in the range 0.1–0.2 eV. (For Si there is a shift of all the couplings toward more favorable ferromagnetic interactions; since Mn-doped Ge is known to be ferromagnetic this suggests that Mn-doped Si might also be—perhaps with a higher Curie temperature).

The coupling between two Mn_{V_2} impurities in diamond is substantially weaker: the largest ferromagnetic couplings are of order 1 meV, two orders of magnitude smaller than for Mn in Ge or Si. Hence, any ferromagnetically ordered phase involving Mn_{V_2} impurities would be characterized by a Curie temperature at most on this scale, i.e. of order 10 K.

VII. SUMMARY

We have shown theoretically that the Mn impurity in diamond is energetically more favorable in the divacancy site than in the substitutional site. The magnetic properties of the divacancy Mn impurity show nearly degenerate low-spin and high-spin configurations; the degeneracy arises from the weak coupling of separate core and valence moments. Divacancy Mn is predicted to be a double acceptor with two hyperdeep levels, suggesting poor prospects for creating the delocalized holes in the valence band that are required to mediate a ferromagnetic interaction within the Zener model. Explicit calculation of the effective Heisenberg coupling between Mn in nearby divacancy sites confirms that Mn-doped diamond shows little promise of ferromagnetism above a few Kelvins.

Our findings may not be unique to diamond: other semiconductors with predicted high Curie temperatures have similarly small atomic volumes, which may likewise make the substitutional site unfavorable for Mn doping. Comprehensive calculations of the site energetics for GaN, ZnO, and other host semiconductors would be of great interest.

VIII. ACKNOWLEDGEMENTS

This work was supported by the Office of Naval Research and the DARPA Spins in Semiconductors program. Computations were performed at the DoD Major Shared Resource Centers at ASC and NAVO.

-
- ¹ H. Ohno, A. Shen, F. Matsukura, A. Oiwa, A. Endo, S. Katsumoto, and Y. Iye, *Appl. Phys. Lett.* **69**, 363 (1996).
 - ² Y. D. Park, A. T. Hanbicki, S. C. Erwin, C. S. Hellberg, J. M. Sullivan, J. E. Mattson, T. F. Ambrose, A. Wilson, G. Spanos, and B. T. Jonker, *Science* **295**, 651 (2002).
 - ³ T. Dietl, H. Ohno, F. Matsukura, J. Cibert, and D. Fermand, *Science* **287**, 1019 (2000).
 - ⁴ T. Dietl, H. Ohno, and F. Matsukura, *Phys. Rev. B* **63**, 195205 (2001).
 - ⁵ S. C. Erwin and C. S. Hellberg, unpublished.
 - ⁶ G. Kresse and J. Hafner, *Phys. Rev. B* **47**, 558 (1993).
 - ⁷ G. Kresse and J. Furthmüller, *Phys. Rev. B* **54**, 11169 (1996).
 - ⁸ G. Makov and M. C. Payne, *Phys. Rev. B* **51**, 4014 (1995).
 - ⁹ S. C. Erwin and A. G. Petukhov, *Phys. Rev. Lett.* **89**, 227201 (2002).
 - ¹⁰ J. P. Goss, R. Jones, S. J. Breuer, P. R. Briddon, and S. Oberg, *Phys. Rev. Lett.* **77**, 3041 (1996).
 - ¹¹ R. Jones, J. E. Lowther, and J. Goss, *Appl. Phys. Lett.* **69**, 2489 (1996).
 - ¹² V. A. Nadolinny, A. P. Yeliseyev, O. P. Yuryeva, and B. N. Feygelson, *Applied Magnetic Resonance* **12**, 543 (1997).
 - ¹³ D. J. Twitchen, J. M. Baker, M. E. Newton, and K. Johnston, *Phys. Rev. B* **61**, 9 (2000).
 - ¹⁴ K. Iakoubovskii, A. Stesmans, B. Nouwen, and G. J. Adriaenssens, *Phys. Rev. B* **62**, 16587 (2000).
 - ¹⁵ G. D. Watkins and J. W. Corbett, *Phys. Rev.* **138**, A543 (1965).
 - ¹⁶ R. G. Humphreys, S. Brand, and M. Jaros, *J. Phys. C* **16**, L337 (1983).
 - ¹⁷ M. Pesola, J. von Boehm, S. Poykko, and R. M. Nieminen, *Phys. Rev. B* **58**, 1106 (1998).
 - ¹⁸ B. J. Coomer, A. Resende, J. P. Goss, R. Jones, S. Oberg, and P. R. Briddon, *Physica B* **273-274**, 520 (1999).
 - ¹⁹ The irreducible representation a_{2u} is sometimes written as a_{1u} in the literature, e.g. Ref. [18].
 - ²⁰ C. A. Coulson and F. P. Larkins, *J. Phys. Chem. Solids* **30**, 1963 (1969).
 - ²¹ S. M. Sze, *Physics of Semiconductor Devices* (John Wiley, New York, 1981).
 - ²² J. Schneider, U. Kaufmann, W. Wilkening, M. Baeumler, and F. Kohl, *Phys. Rev. Lett.* **59**, 240 (1987).